Accepted Manuscript

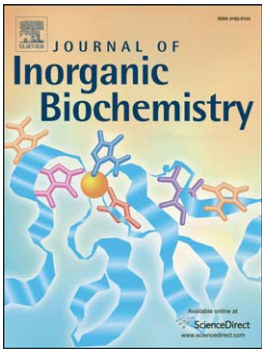

The Heme-Based Oxygen Sensor *Rhizobium etli* FixL: Influence of Auxiliary Ligands on Heme Redox Potential and Implications on the Enzyme Activity

Nathalie Honorio-Felício, Marta S.P. Carepo, Tércio de F. Paulo, Luiz Gonzaga de França Lopes, Eduardo H.S. Sousa, Izaura C.N. Diógenes, Paul V. Bernhardt

PII: S0162-0134(16)30236-7
DOI: doi: 10.1016/j.jinorgbio.2016.08.009
Reference: JIB 10064

To appear in: *Journal of Inorganic Biochemistry*

Received date: 10 May 2016
Revised date: 5 August 2016
Accepted date: 22 August 2016

Please cite this article as: Nathalie Honorio-Felício, Marta S.P. Carepo, Tércio de F. Paulo, Luiz Gonzaga de França Lopes, Eduardo H.S. Sousa, Izaura C.N. Diógenes, Paul V. Bernhardt, The Heme-Based Oxygen Sensor *Rhizobium etli* FixL: Influence of Auxiliary Ligands on Heme Redox Potential and Implications on the Enzyme Activity, *Journal of Inorganic Biochemistry* (2016), doi: 10.1016/j.jinorgbio.2016.08.009

The Heme-Based Oxygen Sensor *Rhizobium etli* FixL: Influence of Auxiliary Ligands on Heme Redox Potential and Implications on the Enzyme Activity

Nathalie Honorio-Felício[a,b], Marta S. P. Carepo[a], Tércio de F. Paulo[a], Luiz Gonzaga de França Lopes[a], Eduardo H. S. Sousa[a*], Izaura C. N. Diógenes[a*]

[a]Laboratório de Bioinorgânica, Departamento de Química Orgânica e Inorgânica, Universidade Federal do Ceará, CEP 60455-760, Fortaleza, Ceará, Brazil.

izaura@dqoi.ufc.br; eduardohss@dqoi.ufc.br

Paul V. Bernhardt[b]*

[b]School of Chemistry and Molecular Biosciences, The University of Queensland, Brisbane-QLD, 4072, Australia.

p.bernhardt@uq.edu.au

Abstract

Conformational changes associated to sensing mechanisms of heme-based protein sensors are a key molecular event that seems to modulate not only the protein activity but also the potential of the $Fe^{III/II}$ redox couple of the heme domain. In this work, midpoint potentials (E_m) assigned to the $Fe^{III/II}$ redox couple of the heme domain of FixL from *Rhizobium etli* (*Re*FixL) in the unliganded and liganded states were determined by spectroelectrochemistry in the presence of inorganic mediators. In comparison to the unliganded *Re*FixL protein (+19 mV), the binding to ligands that switch off the kinase activity induces a negative shift, i. e. E_m = –51, –57 and –156 mV for O_2, imidazole and CN^-, respectively. Upon binding to CO, which does not affect the kinase active, E_m was observed at +21 mV. The potential values observed for $Fe^{III/II}$ of the heme domain of *Re*FixL upon binding to CO and O_2 do not follow the expected trend based on thermodynamics, assuming that positive potential shift would be expected for ligands that bind to and therefore stabilize the Fe^{II} state. Our results suggest that the conformational changes that switch off kinase activity upon O_2 binding have knock-on effects to the local environment of the heme, such as solvent rearrangement, destabilize the Fe^{II} state and counterbalances the Fe^{II}-stabilizing influence of the O_2 ligand.

Keywords: Heme-based sensor, FixL, redox potential, kinase activity, spectroelectrochemistry

1. Introduction

During the last two decades, a new family of hemoproteins has emerged with the function of biological sensors. Currently, these proteins are called heme-based sensors and are ubiquitous in nature; from archae to humans. These sensors have also exhibited many distinct biological functions, such as regulators of nitrogen fixation, aerotaxis, dormancy, circadian rhythms, among others [1-4]. Interestingly, these proteins harbour the heme group in at least 7 different types of fold, e.g. PAS, Globin, CooA, HNOB, GAF, SCHIC, LDB, which are usually coupled to a variety of output domains, including domains that exhibit enzymatic activity, DNA-protein or protein-protein interaction properties under ON/OFF control by the axial ligands bound to the heme domain [2, 3], as schematically illustrated in Fig. 1.

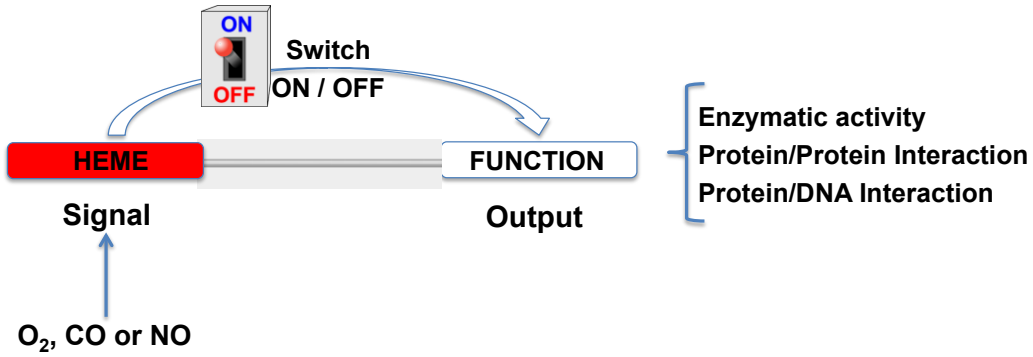

Fig. 1. General Scheme of Heme-Based Sensor Regulation

In 1991, a landmark publication reported that FixL was an oxygen heme-based sensor [5]. Since then, FixL has been one of the most thoroughly investigated heme-based sensors, with many of its mechanistic details elucidated [6-14]. Commonly found in bacteria, FixL is part of a two-component system in which it acts as a sensor kinase while the transcription factor FixJ acts as a response regulator protein [15]. While the kinase activity of FixL is switched off upon binding to O_2 [8, 16], under anaerobiosis a FixL histidine residue is autophosphorylated. Subsequent transfer of the histidine

phosphoryl group to an aspartate residue in the N-terminal signaling domain of FixJ makes the transcriptionally active phospho-FixJ, which then induces the expression of nitrogen fixation and microaerobic respiration genes (*fix* and *nif* genes) [3].

FixL from *Bradyrhizobium japonicum* (*Bj*FixL) and *Sinorhizobium meliloti* (*Rm*FixL) have been widely studied over recent years and, despite the fact that these FixLs are quite similar (see sequence alignment in Fig. S1 of the Supplementary Material), there are some differences in their domain organization and heme-regulated properties [6-10, 12-14]. For example, *Bj*FixL can catalyse FixJ phosphorylation either in the deoxy (Fe^{II}) or met (Fe^{III}) state, while oxy (Fe^{II}-O_2) and cyano-met (Fe^{III}-CN^-) states efficiently deactivate *Bj*FixL. On the other hand, *Rm*FixL is only fully active in the deoxy (Fe^{II}) state, while met (Fe^{III}), oxy (Fe^{II}-O_2) and cyano-met (Fe^{III}-CN^-) states are kinase inactive towards FixJ turnover. Recently, another interesting FixL from *Rhizobium etli* (*Re*FixL) was investigated [11]. This is a hybrid sensor kinase that contains, additionally to *Bj*FixL domains, a FixJ-like receiver domain at the C-terminal. This system promotes histidine phosphorylation and phosphoryl transfer to aspartate in the same protein, which facilitates investigation of all of these regulatory phenomena in one protein. Similarly to *Bj*FixL, *Re*FixL contains two PAS domains in tandem and is fully kinase active in the deoxy (Fe^{II}) and met (Fe^{III}) states while bound to O_2 and CN^-, the *Re*FixL protein is no longer active. The heme is bound to the second PAS domain, while the first PAS also mediates signal transduction and influences the oxygen affinity of the second PAS. *Re*FixL has the lowest oxygen affinity measured for any heme based sensor (K_d = 738 μM) [11]. Nevertheless, the kinase activity of *Re*FixL is fully inhibited when only 26% of the protein is saturated with oxygen; since *Re*FixL is dimeric, cooperativity cannot account for this. The most likely explanation is a hysteretic effect similar to the "memory effect" shown for *Bj*FixL [12].

In heme-based sensors, as in all other ligand binding heme proteins, amino acid residues in contact with the heme are sensitive to ligand binding. These local structural changes and their accompanying effects on reduction potential have been measured for some heme based sensors. [17]. For FixL proteins, however, only a few studies on the redox potentials have been conducted, and only with isolated heme domains, not the full-length protein, which will miss all the effects due to coupling of the heme domain changes to the conformational changes in the kinase domain that result in reversible inactivation. [17-20]. These long-range effects of ligand binding are broadly analogous to the triggering of the R-T quaternary structure change in hemoglobin caused by ligand binding. Such changes must affect the redox potential making the understanding of this connection a key step for learning the mechanistic principles of signal transduction.

In this work we have examined the full-length *Re*FixL at different liganded states and conditions using mediated spectroelectrochemistry, where the protein is gradually reduced/oxidized at a constant applied potential and a spectrum is recorded for each potential. To ensure equilibrium is established between the electrode and the oxidized and reduced forms of FixL small molecular weight redox mediators are present as electron relays between the electrode and the protein.

2. Materials and Methods

2.1. Chemicals

Aqueous solutions were prepared using Millipore (Germany) water of resistivity greater than 18.2 MΩ cm at 25 ^{o}C. Tris(hydroxymethyl)aminomethane, sulfuric acid, formic acid, acetic acid, imidazole, NaCl, all from Sigma-Aldrich (United States), and KCN from Merck (Germany) were used as received.

The mediator 2,5-dihydroxybenzoquinone [21] was purchased from Lancaster and the following coordination compounds (with their formal $Co^{III/II}$ redox potentials at pH 8.0) $[Co((NMe_3)_2sar)]Cl_5$ (+10 mV vs NHE), $[Co(CLME\text{-}N_4S_2\text{-}sar)]Cl_3$ (–134 mV vs NHE), $[Co(AMME\text{-}N_5S\text{-}sar)]Cl_3$ (–220 mV vs NHE), $[Co(sep)]Cl_3$ (–296 mV vs NHE), $[Co(AMMEsar)]Cl_3$ (–380 mV vs NHE) and $[Co(trans\text{-}diammac)](ClO_4)_3$ (–551 mV vs NHE) have been described collectively in earlier publications [22-27].

2.2. Protein Expression, Purification and Assays

The full-length *Rhizobium etli fixL* (*Re*FixL) gene was cloned in a pUC19 derived plasmid under a tac promoter regulation, which contained ampicillin resistance gene for selection in *Escherichia coli* strain MC1061*(E. coli)*. The expression and purification followed the procedures described in the literature [11]. The purity of the protein was evaluated by SDS-PAGE and UV-Vis spectra resulting in > 90%.

2.3. Spectroelectrochemistry

Spectroelectrochemistry measurements were performed with a BAS100B/W or EPSILON potentiostats (Bioanalytical Systems Inc., BASi, West Lafayettte, IN, USA) using an optically transparent thin-layer cell (OTTLE, 0.1mm or 0.05 mm) with a gold or platinum mesh working electrode, a platinum wire counter electrode and Ag/AgCl reference electrode (+196 mV vs NHE), in conjunction with an Ocean Optics USB2000 fibre optic UV-Vis spectrophotometer (United States) with the spectroelectrochemistry cell mounted inside a Belle Technology anaerobic box (O_2 concentration < 20 ppm, United Kingdom). For experiments performed in the presence of oxygen the buffer solution (35 mM Tris, pH 8.0, 100 mM NaCl) was previously saturated with pure O_2 for 20 min and a constant flux was kept during the titrations. A Cary 5000 UV-Vis-NIR (United States) and an Agilent 8453 diode array spectrophotometers (United States) were used for the acquisition of the spectra with applied potential. While the

measurements in the presence of O_2 and CN^- were taken on the former equipment, the Agilent spectrophotometer was used for the acquisition of the spectra in air and in the presence of CO.

All potentials, unless otherwise specified, are referenced against a normal hydrogen electrode (NHE) at room temperature (25˚C) and the Ag|AgCl/Cl^- reference electrode was always calibrated against the quinhydrone redox couple (+86 mV vs Ag|AgCl/Cl^- at pH 7.0 and 25˚C).

Typical spectroelectrochemical experiments were run with *ca.* 15 µM of *Re*FixL in an electrolyte solution of 35 mM Tris buffer (pH 8.0) and 100 mM NaCl. All mediators, except 2,5-dihydroxybenzoquinone, which was used only in the anaerobic study of *Re*FixL with no additional ligands, were used at concentrations of *ca.* 100 µM. Prior to the acquisition of the spectra, the working electrode (Au mesh or Pt mesh) was polarized at + 0.3 V vs NHE for 8 min to ensure the fully oxidized state of the protein, met-*Re*FixL (Fe^{III}-unliganded *Re*FixL). Typically, the potential was scanned firstly in the negative direction and then back in the positive direction to check the reversibility of the systems and the existence of hysteresis. A potential range of 0.55 V, usually from +0.3 to −0.25V vs NHE, was applied in steps of 0.05V and 0.025V in the vicinity of the redox midpoint potential. Each potential was held for at least 8 min before the spectrum was taken. All data were treated by global analysis with Reactlab Redox (Australia) [28] and kinetic analysis of the spectral changes as a function of time was performed with Reactlab Kinetics (Australia) [29].

3. Results

Aiming to study the redox process of the *Rhizobium etli* FixL (*Re*FixL) protein in the presence of O_2, CO, CN^-, and imidazole, a series of spectroelectrochemical measurements were conducted using a mixture of the mediators given in the Section 2.1. The organic mediator 2,5-dihydroxybenzoquinone (−60 mV vs NHE) was also used in the measurements of *Re*FixL in deaerated solution to provide additional redox buffering at higher potentials. In this work, a mixture of all mediators were used in each experiment to provide identical conditions in each case regardless of where the redox potential was found in *Re*FixL. As reported previously [30], relative to the strongly absorbing heme chromophore (at a concentration of 15 μM), the Co complex mediators are essentially colorless in both oxidation states at the concentrations used (100 μM) as so no interference from mediator absorption is found.

We initially found that experiments in the presence of CN^- carried out with a gold working electrode were not reversible as the concentration of CN^- in solution decreased during the course of the experiment. This was attributed to the anodic formation of $[Au(CN)_2]^-$ and thus consumption of the cyanide. This problem was averted by using a Pt mesh working electrode as Pt is inert to oxidation in the presence of cyanide at the potentials used in the experiment. Also, CN^- is a weak base (pK_a 9.2) so experiments with this ligand were carried out at pH 9.5 to avoid major protonation and loss of volatile HCN from the solution. In order to discuss the data obtained for *Re*FixL-CN^- in relation to the unliganded protein, the spectroelectrochemical experiments for the deoxy-*Re*FixL were also performed at pH 9.5.

Fig. 2A shows the spectral results for the oxidized (Fe^{III}) and reduced (Fe^{II}) forms of *Re*FixL in the absence of oxygen. Global analysis of all absorbance/wavelength data obtained across all applied potentials (see Figs S2 to S6 in

the Supplementary Material) yielded the redox midpoint potential of the half reaction and also the spectra of the fully oxidized and reduced forms, as shown in Fig. 2.

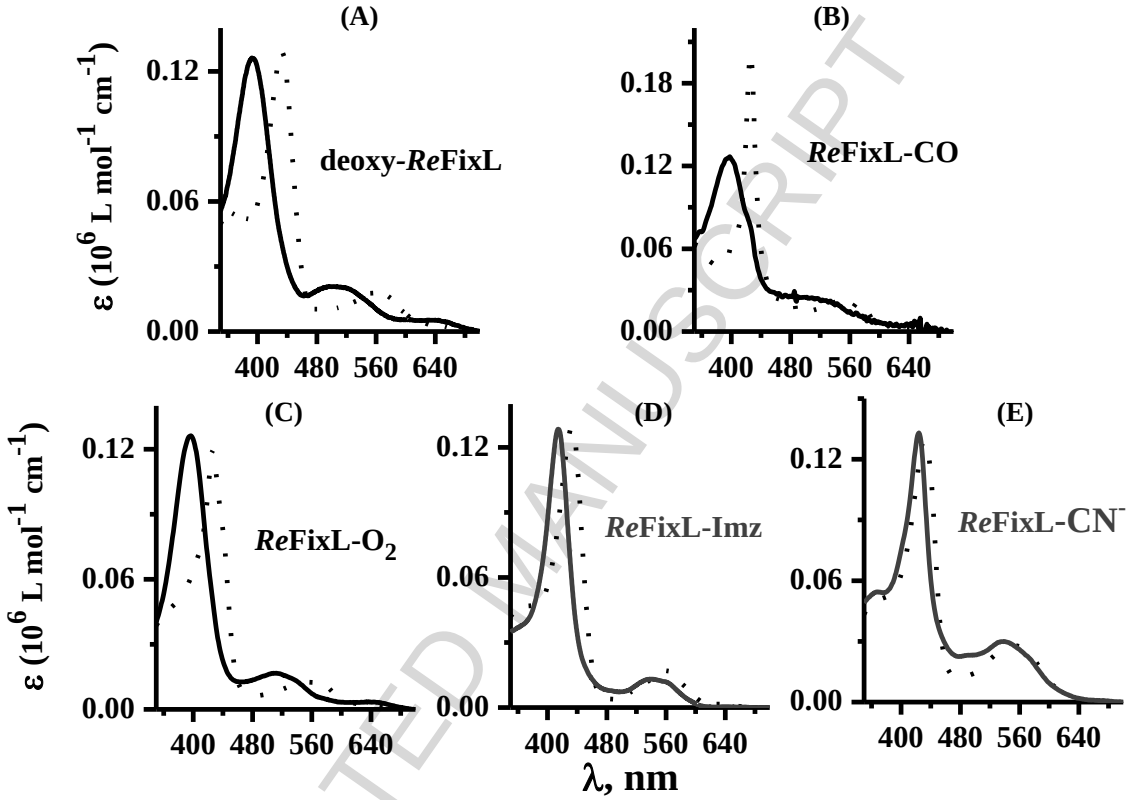

Fig. 2. UV-Vis spectra of the unliganded Fe^{III} (solid black line), Fe^{III}-imz and Fe^{III}-CN (dark gray line), and Fe^{II} (dotted black line) forms of 15 μM *Re*FixL in electrolyte solutions (35 mM Tris buffer (pH 8.0) and 100 mM NaCl) as follows: (A) deoxygenated, (B) CO saturated (0.93 mM), (C) oxygen saturated (1.25 mM, at 25 ^oC), (D) 200 mM imidazole and (E) 1.0 mM CN^- (pH 9.5).

In the absence of any additional ligands, the spectra in Fig. 2A are each characteristic of the five-coordinate deoxy-Fe^{II} and Fe^{III} states of the *Re*FixL heme [30]. The most pronounced change is in the Soret band, which shifts from 395 nm (Fe^{III}) to 432 nm (Fe^{II}). The broad visible absorption band (a combination of the α- and β-bands) also shifts to longer wavelength upon reduction (500 nm to 560nm).

It is well known that CO is a ligand that binds very well to heme cofactors, binding only to the Fe^{II} heme similar to oxygen. We also found this with *Re*FixL (Fig. 2B), where an intense and sharp Soret band (426 nm) for the six-coordinate Fe^{II}-CO, *Re*FixL-CO, form was identified. Also the α- and β- bands are well resolved as maxima at 571 and 542 nm, respectively. As expected the Fe^{III} heme is unaffected by CO and the same spectrum of the five-coordinate Fe^{III} heme seen in Figs 2A and 2B is obtained.

In the presence of oxygen (Fig. 2C) the spectral changes are subtly different. Initially the Fe^{III} spectrum is the same as in Fig. 2A as the Fe^{III} heme has no affinity for oxygen. However, O_2 does bind to the Fe^{II} heme and the spectrum of the oxy-Fe^{II} form (Fig. 2C) is clearly different from the deoxy-Fe^{II} state (Fig. 2A). The most significant change is the splitting of the single visible region band of deoxy-Fe^{II} (Fig. 2A) into two broad peaks at 569 and 554 nm. It should be mentioned that the calculated spectrum of the oxy-Fe^{II} form is actually a combination of deoxy-Fe^{II} and oxy-Fe^{II} as the heme cofactor has only a weak affinity for dioxygen; i.e. *c.a.* 26% and 63% oxygen bound in air and under O_2 saturation, respectively [11].

In Fig. 2D, the spectra are in the presence of 200 mM imidazole. The Fe^{III} spectrum is clearly different from those of the five-coordinated Fe^{III} heme (Figs 2A and 2B) and indicate that imidazole is coordinated *trans* to the histidine residue ligand in the axial coordination site *i.e.* a six-coordinated Fe^{III} heme, *Re*FixL-imz. The Soret band sharpens, gains intensity and moves to longer wavelength. By contrast the Fe^{II} spectrum is identical to that determined in the absence of any ligands and without oxygen present (Fig. 2A), so imidazole is not bound in the Fe^{II} state.

Cyanide is a very effective ligand that prefers Fe^{III} over Fe^{II} heme. In the presence of 1 mM CN^- the Soret band of the Fe^{III} heme in *Re*FixL shifts immediately from 395 nm to 421 nm corresponding to a change from five-coordinate to six-

coordinate Fe^{III}-CN heme, *Re*FixL-CN. Upon reduction the CN^- ligand is lost (Fig. 2E) as the spectrum is again identical to the deoxy-Fe^{II} spectrum seen in Figs 2A and 2D.

In all cases the spectra were reversible and it did not matter whether the spectra were acquired starting from a high (Fe^{III}) or low (Fe^{II}) potential. The calculated spectra were the same and the redox potentials obtained from the reductive or oxidative sweeps were identical; i.e. no relevant hysteresis was seen. In principle only the redox potential of the deoxy-$Fe^{III/II}$ can be considered a formal potential as there is no change in coordination number. All of the redox potentials calculated from the data in Figs 2B-2E are electron transfer reactions coupled to chemical reactions, e.g. Fe(III)—L + e^- $\rightleftharpoons$ Fe(II) + L (L = CN^- and imz) or Fe(III) + L' + e^- $\rightleftharpoons$ Fe(II)—L' (L' = O_2 and CO). These coupled chemical reactions (ligand binding) were fast on the timescale of the spectroelectrochemical cell but the determined midpoint potentials (E_m) obtained from the experiments involving ligand binding to either Fe^{III} or Fe^{II} are necessarily shifted from the formal potential. Usually, ligand binding to the Fe^{III} state (but not to the Fe^{II} state) should result in a negative shift in the redox potential and ligand binding exclusively to the Fe^{II} state should result in a positive shift. This was not always seen (Table 1) and an explanation of these interesting changes in the redox potentials is deferred to the Discussion.

Table 1. Midpoint potentials (E_m, mV *vs* NHE), shifts of the liganded E_m values in relation to the non-bounded *Re*FixL (ΔE_m, mV) and Soret band electronic spectral maxima (λ in nm and ε in mM cm^{-1}) of Fe^{III} and Fe^{II} *Re*FixL in its various liganded states.

Protein	[a]E_m	ΔE_m	**Fe^{III}**		**Fe^{II}**	
			λ_{ox}	**ε**	λ_{red}	**ε**
*Re*FixL	+19.0 ± 11	0.0	395	126.0	432	129.2
[b]*Re*FixL	−11 ± 2.8	-	395	126.0	432	129.2
*Re*FixL-O_2 (air)	−12 ± 8	−31.0	395	126.0	428	134.5
*Re*FixL-O_2 (O_2 saturated solution)	−51 ± 10	−70.0	395	126.0	426	134.5
*Re*FixL-CO	+21 ± 1.6	2.0	395	126.0	426	201.7
*Re*FixL-imz	−57 ± 10	−76.0	415	128.4	432	129.2
[b]*Re*FixL-CN	−156 ± 4.9	−145.0[c]	424	148.4	432	129.2

[a]Fe(III)—L + e^- $\rightleftharpoons$ Fe(II) + L (L = CN^- and imz) or Fe(III) + L' + e^- $\rightleftharpoons$ Fe(II)—L' (L' = O_2 and CO). [b]Measurements at pH 9.5. [c]ΔE_m value was calculated based on the E_m value determined for *Re*FixL (E_m = −11 mV) at pH 9.5.

4. Discussion

4.1. Optical Spectral Features of ReFixL in its Oxidized and Reduced Forms

The spectral dependence of the liganded and unliganded *Re*FixL protein on the applied potential always gave series of spectra with well-defined isosbestic points (Figs. S2 to S6 of the Supplementary Material) supporting the interchange of only two redox active species. The only exception to this was for the oxy-Fe^{II} form of *Re*FixL which was always in equilibrium with its deoxy-Fe^{II} form due to its known weak affinity for

oxygen. In fact the calculated spectrum of 'oxy-Fe^{II}' *Re*FixL is a mixture of both oxy- and deoxy-Fe^{II}.

Upon reduction of Fe^{III} to Fe^{II} heme, the Soret maximum of the fully oxidized state of *Re*FixL, met-*Re*FixL, shifts from 395 to 432 nm (Fig. 2A) while the combined maximum of the broad α/β bands shift from 500 to 563 nm, a behavior consistent with five coordinate, high-spin, *b*-type hemes [31, 32]. In oxygen saturated solution (Fig. 2C), the Soret band presents a similar shift upon reduction. The shape of the band, however, is broad and asymmetric supporting partial formation of oxy-*Re*FixL as previously reported [11].

A hypothetical domain-domain response induced by the binding of small molecules to the PAS domain of *Re*FixL was raised in the literature based on the changes in oxygen affinity modulated by the adjacent non-heme-binding PAS domain [11]. Similar behavior was reported before for other heme-based sensors [33, 34], where oxygen affinity for the heme domains and full-length proteins showed significant differences. Full-length *Bj*FixL showed a 4-fold lower oxygen affinity than its isolated heme domain, while DosP, an oxygen sensor phosphodiesterase, was 6-fold lower [33, 34]. These results have highlighted the sensitivity and connectivity of the heme to changes also outside of the immediate vicinity of the iron heme, which can occur during signal transduction events. Furthermore, these observations reinforce the importance of measurements conducted on the full-length protein.

Such findings lead us to surmise that the redox behavior and, consequently, the physiological function of *Re*FixL is affected by binding other small molecules such as CO, imidazole and CN^-. Figs 2B, 2D and 2E show the spectral changes of *Re*FixL with applied potential in solution containing CO, imidazole and CN^-, respectively. In solutions containing imidazole and CN^-, the Soret band of the met-*Re*FixL shifts to 415

nm and 424 nm (Figs. 2D and 2E), respectively, indicating binding to Fe^{III}. On the other hand, no shift is observed in the spectra of met-*Re*FixL in the CO saturated medium (Fig. 2B). In the presence of CO, the Soret band of the Fe^{II} form shifts to 426 nm along with a concomitant shape change to a sharp and very intense peak. This is corroborated by clear separation of the α- and β-band maxima which also indicates the CO coordination in the sixth site; features characteristic of low spin Fe^{II} heme *b* chromophores. In the imidazole and cyanide experiments, the oxidative scan leads to the recovery of the non-CO-coordinated form.

4.2. Ligand Dependent Shifts in Redox Potential

For discussion purpose, Table 2 displays the E_m values for the systems studied in this work along with those reported in the literature for some sensor and non-sensor heme-based proteins.

Table 2. Redox potentials of sensor and non-sensor heme-based proteins.

Heme protein	E_m, mV	Reference
PAS domain		
*Re*FixL	+19	This work
*Re*FixL*	−11	This work
*Re*FixL-O_2 (air)	−12	This work
*Re*FixL-O_2 (O_2 saturated solution)	−51	This work
*Re*FixL-CO	+21	This work
*Re*FixL-imz	−57	This work
*Re*FixL-CN*	−156	This work
*Bj*FixL	+68	[18]

DosP (EcDOS)	+67	[19, 35, 36]
Globin domain		
DosC (YddV) (Globin)	–22	[20]
HNOB domain		
sGC (*Manduca sexta)*	+234	[37]
sGC *Bovine*	+187	[38]
Cyt c domain		
DcrA-N	–250	[39]
GSU582	–156	[40]
GSU935	–251	[40]
Non-sensor heme proteins		
Myoglobin	46	[41]
Myoglobin – CN	–385	[41]
Cytochrome P450 CYP2C9	–41	[42]
Cytochrome P450 CYP2C9 – CO	+8	[42]
Cytochrome P450 CYP2C9 – O_2	+9	[42]
PSM	–283	[43]
PSM – CO	0.0	[43]
Microperoxidase-8	-139	[44]
Microperoxidase-8 – CN	-176	[44]
Microperoxidase-8 – imz	-203	[44]

*Measurements at pH 9.5

The unliganded *Re*FixL presents a $Fe^{III/II}$ redox potential significantly lower than *Bj*FixL (+68 mV) and DosP (+67 mV), where the heme is also harbored in a PAS

domain. It is worth mention that, like *Bj*FixL, the unliganded *Re*FixL is kinase active in both iron states (Fe^{II} and Fe^{III}) [11].

The significant negative shifts of the redox potentials (ΔE_m, Table 1) in the presence of imidazole and CN^- are consistent with thermodynamic predictions, where ligand binding to the higher oxidation state more tightly than the lower oxidation state elicits a negative shift in the observed midpoint potential; the shift being related to the relative ligand binding constants in the oxidized and reduced states. The larger shift in the cyanide experiment (ΔE_m −145 mV) compared with imidazole (ΔE_m −76 mV) reflects a greater (almost hundred-fold) Fe^{III}-CN binding constant than with imidazole. It should be addressed that the ΔE_m value of *Re*FixL-CN^- was calculated based on the E_m values determined for both *Re*FixL-CN^- and *Re*FixL (E_m = −11 mV) at pH 9.5. In fact, CN^- ligand showed much larger affinity (over 100-fold) than imidazole to *Bj*FixL and *Rm*FixL [7, 43], whose trend is followed by *Re*FixL as indicated by the reported k_{on} rates [11].

Following the reasoning above, the coordination of ligands high in the spectrochemical series (CO, CN^-, imidazole) to the lower oxidation state, on the other hand, would result in positive potential shift due to thermodynamic stabilization of the Fe^{II} states of the protein. Cytochrome P450 CYP2C9 (Fe^{II}), for instance, upon binding to CO shows a positive shift of 49 mV relative to the non-CO bound protein [42]. Another small peptide model of hemoproteins, called peptide-sandwiched mesoheme (PSM), exhibits an even larger potential shift (c.a. 283 mV) upon binding to CO [44]. Contrary to such thermodynamic predictions, for the *Re*FixL protein, CO does not alter the midpoint potential of the heme significantly from the unliganded form (ΔE_m +2 mV). A similar observation was found for the spectroelectrochemical experiment performed in the presence of O_2. Oxygen binding exclusively to the Fe^{II} heme should

also elicit a positive shift in the $Fe^{III/II}$ redox potential but the opposite was found (ΔE_m −70 mV). Furthermore, the actual shift is almost certainly underestimated as the oxygen binding was incomplete. In fact, in air, where only 26% of oxygen bound is reported [11], the value of E_m was observed at −12 mV with a potential shift of −31 mV in relation to deoxy-*Re*FixL (Fig. S7 of the Supplementary Material).

4.3. Structural Changes Upon Ligand Binding

There are clearly other effects at play that counterbalance the ligand-binding positive shifts in $Fe^{III/II}$ redox potential for CO and O_2. There are reports of redox potential changes upon ligand binding that do not involve coordination to the metal center but instead induce a conformational change in the protein. Soluble guanylate cyclase from *Manduca sexta* showed a consistent positive shift of +22 mV upon binding to YC-1, an allosteric effect that affects heme regulation but does not bind to the iron [37]. As mentioned above, modifications to the protein secondary structure may have knock-on effects to the local environment of the heme that lead to different second sphere interactions at the active site, i.e. ligand binding has indirect effect on the protein structure. We suggest that similar events may occur here. Despite the lack of full-length X-ray structure for FixL, there is a variety of heme domain structures published for FixL from *Sinorhizobium meliloti* and *Bradyrhizobium japonicum* in the Fe^{II} unliganded (Fe^{II}), carbonyl (Fe^{II}-CO), and nitrosyl (Fe^{II}-NO) in addition to the Fe^{III} unliganded (Fe^{III}), cyano (Fe^{III}-CN^-) and imidazole (Fe^{III}-imz) bound forms [14, 46-50]. We have focused on the most relevant amino acids (within 7 Å of the Fe atom) as shown in Figs 3 and 4. The CO-bound *Bj*FixL protein has been crystallized in three different space groups *R*32 (one independent molecule in the asymmetric unit), *C*2 (2 independent molecules) and *P*1 (four independent molecules); so there are 7 independent structures of the heme active site. Fig. 3A shows one of these 7 CO-bound structures and three

hydrophobic residues (Ile215, Ile238 and Leu236) are highlighted. These alkyl side chains have conformational flexibility but in the case of CO-bound *Bj*FixL, remarkably, 6 of the 7 heme structures bear different conformational combinations of these three hydrophobic residues. This reveals a large degree of conformational flexibility at the active site of CO-bound *Bj*FixL and uncertainty in the actual solution structure. By contrast the Fe^{III} heme structure of *Bj*FixL is more rigid; 5 independent heme domains have been structurally characterized and 4 of them are found in the conformation shown in Fig. 3B. If these structures can be taken to be representative of solution behavior then there is a large conformational rearrangement of the hydrophobic Ile and Leu residues upon oxidation of the Fe^{II}-CO form to met-Fe^{III}. Such changes may be correlated with solvent rearrangement at the active site that stabilizes the Fe^{III} form and counterbalances the Fe^{II}-stabilizing influence of the CO ligand. An overlay view of the X-ray structures of the heme domains is shown in Fig. S8 of the Supplementary Material, where the conformational changes can be better visualized.

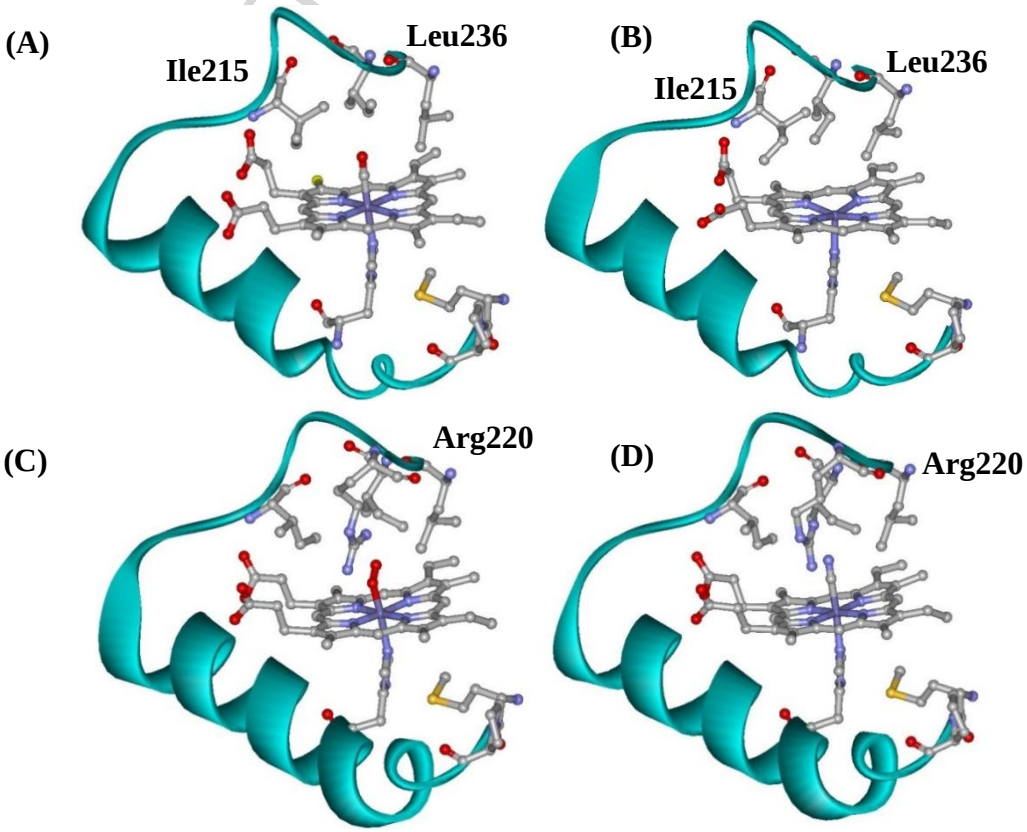

Fig. 3. Crystal structures of *Bj*FixL (**A**) in one of its CO-bound forms (PDB 1XJ2), (**B**) in its Fe^{III} unliganded state (PDB 2VV6), (**C**) in its O_2-bound forms (PDB 1DP6) and (**D**) in its Fe^{III} CN^- bound state (PDB 1LT0).

The conformational change in *Bj*FixL upon oxygen binding is even more dramatic. As shown in Fig. 3(C), O_2 binding is accompanied by appearance of an arginine residue (Arg220) that is in H-bonding contact with the dioxygen ligand. The movement of Arg220 has an even more significant effect on the secondary structure of the protein. Taking a wider view of the structure (Fig. 4), in the absence of dioxygen as a ligand, Arg220 swings away from the heme pocket and H-bonds to a heme propionate and a number of other H-bonding interactions are disturbed. This Arg220 was showed to play a key role not only in ligand binding, but also critically on signal transduction along with Arg206. These interactions cause heme distortion and affect heme propionate, which has also been noticed in other heme-based sensor signal transduction event [17]. Distal hydrophobic residues Leu and Ile, previously described, have also a role as steric residues implicated in the signal transduction as reported elsewhere [48], which might have an important role particularly upon imidazole binding.

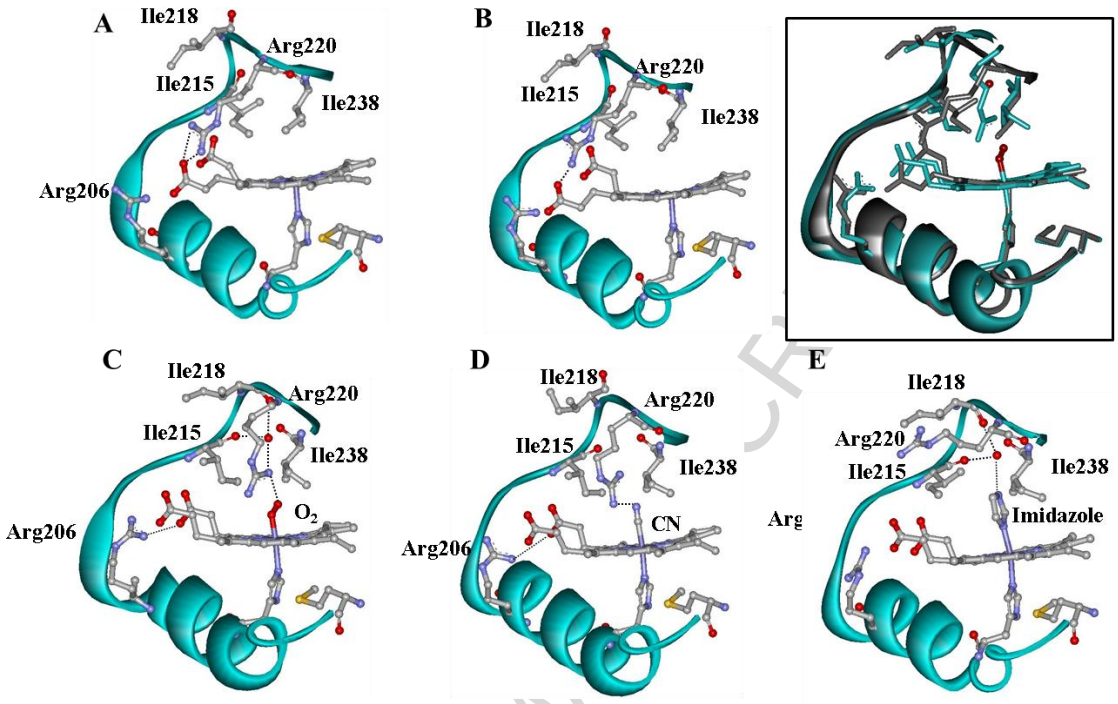

Fig. 4. X-ray crystal structures of the heme domain of *Bj*FixL in the (A) Fe^{III} form (PDB 1DRM), (B) Fe^{II} deoxy form (PDB 1LSW), (C) Fe^{II} oxy form (PDB 1DP6), (D) Fe^{III} cyanide bound form (PDB 1LT0) and (E) Fe^{III} imidazole bound form (PDB 1DP9) illustrating the changes in protein conformation upon O_2, cyanide and imidazole binding. Inset: superimposed structures of Fe^{II} oxy (blue) and deoxy (grey) *Bj*FixL.

As expected, the same inactive site conformation has been observed in the Fe^{III} cyanide-bound form of *Bj*FixL where the arginine H-bonds with the cyanide ligand (Fig. 4) [47]. It is known that both the oxy and cyanide bound forms of *Re*FixL are switched off with respect to kinase activity. Accounting for all the crystal structures determined for liganded *Bj*FixL with species relevant to this study, those structures reported for imidazole, O_2 and CN^- ligands exhibit the largest conformational changes [47].

Our results support that electronic properties of the heme are not only dependent on the immediate sixth ligand, but a combination of effects including heme distortion,

nature of microenvironment, propionate ionic interactions, among other effects (steric side chain) as previously suggested by the literature [2, 51, 52]. In summary, there is an overall change upon oxygen binding/release involving FG-loop movement that cause heme to be flatten and movement of hydrophobic distal residues (Ile215, Ile238) along with reorganization of polar residues (especially Arg220). All of these effects counteract the intrinsic positive shift in redox potential upon oxygen binding to Fe^{II}.

4.4. Electrochemical Potential Trend and Kinase Activity

The key process for FixL to work as a heme-based sensor is to bind and recognize selectively a given signal. *Re*FixL in the Fe^{II} state binds very well CO and NO, but none of them can alter histidine kinase activity of this protein [11]. Upon oxygen binding, the histidine kinase activity is switched off, which is due to structural changes started at the heme domain (Fig. 4). On the other hand, *Re*FixL in the Fe^{III} state presents histidine kinase activity, which is likely due to structural similarity of the heme domain of the Fe^{II} state as indicated in Fig. 4 by the X-ray structures of FixLs. In the Fe^{III} state, also, *Re*FixL can be switched off upon binding to CN^- and imidazole, which is in agreement to structural changes noticed at the heme domain. By correlating the histidine kinase activity with the reported overall structural changes of FixL in unliganded and liganded states [47], one can hypothesize the dependence of the electrochemical potentials on the activity of the protein. Having this in mind the terms "ON" and "OFF" in Fig. 5 are related to the kinase activity of the proteins studied in this work. Such evidence is quite interesting because, in certain cases, the electrochemical potential trend does not follow the expected ligand effect on heme, reinforcing other changes taking place to modulate the potential.

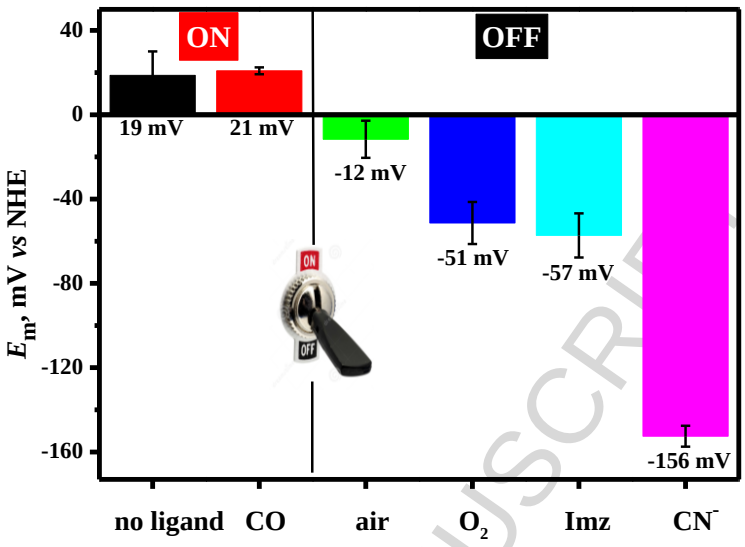

Fig. 5. Bar plot showing the correlation between histidine kinase activity and $Fe^{III/II}$ redox potentials of liganded and unliganded *Re*FixL.

As can be ascertained from Fig. 5, histidine kinase activity is active when the protein shows positive (and quite similar) potentials, i.e. for the unliganded *Re*FixL and *Re*FixL-CO. For *Re*FixL-O_2, *Re*FixL-CN^- and *Re*FixL-imz, whose potentials are all negative, the histidine kinase is switched off.

5. Conclusions

Spectroelectrochemical studies were performed for the unliganded *Re*FixL protein and upon binding to O_2, imidazole, CN^- and CO ligands, knowing that the binding of the first three species switches off the kinase activity of *Re*FixL. In comparison to the unliganded *Re*FixL protein (E_m = +19 mV), the binding to the ligands that switch off the protein induces a negative shift of the midpoint potential (*E*m), i. e. E_m = –51 mV, –57 mV and –156 mV for O_2, imidazole and CN^-, respectively. Upon binding to CO, which does not affect the kinase active, the midpoint potential is

observed at +21 mV. The spectral profiles obtained during applying potential also showed that imidazole and CN^- bind Fe^{III} while O_2 and CO coordinate to Fe^{II}. From a thermodynamic standpoint, the potential of the $Fe^{III/II}$ redox pair would shift negatively upon coordination to iron(III) while a positive shift would be expected upon binding of π acceptor ligands to iron(II) due to the stabilization of the reduced state. Whether the negative shift is indeed observed upon coordination of imidazole and CN^- to Fe^{III}, the binding to Fe^{II} virtually does not affect the redox potential in the case of CO and, most unexpected, shifts the potential negatively upon coordination to O_2, where there are significant changes around heme. Our results, however, supports electronic properties of the heme are not only dependent on the immediate sixth ligand, but a combination of effects including heme distortion and propionate interactions. We can conclude, therefore, that new microenvironment created upon binding to the studied ligands strongly control the overall potential trend, which shown to be correlated to histidine kinase activity of *Re*FixL.

Abbreviations: *Bj*FixL, *Bradyrhizobium japonicum* FixL; *Re*FixL, *Rhizobium etli* FixL; deoxy-*Re*FixL, Fe^{II} unliganded FixL; *Re*FixL-O_2, Fe^{II}-O_2 FixL; *Re*FixL-CO, Fe^{II}-CO FixL; met-*Re*FixL, Fe^{III} unliganded FixL; *Re*FixL-CN, Fe^{III}-cyanide FixL; *Re*FixL-imz, Fe^{III}-imidazole FixL,; imz, imidazole; Fe^{II}, protoporphyrin IX-Fe^{II} complex; Fe^{III}, protoporphyrin IX-Fe^{III} complex; NHE, normal hydrogen electrode; PAS, **P**er, **A**RNT, and **S**im proteins domain; GAF, c**G**MP-specific and stimulated phosphodiesterases, **a**denylate cyclases, and E. coli **f**ormate hydrogen lyase transcriptional activator domain; SCHIC, **s**ensor **c**ontaining **h**eme **i**nstead of **c**obalamin domain; HNOB, **h**eme-**NO**-

binding domain; LBD, **l**igand **b**inding **d**omain for nuclear receptors; CooA, CO sensor transcriptional regulator.

Acknowledgements

I.C.N. Diógenes (# 304285/2014-5), E.H.S. Silva (# 312030/2015-0), L.G.F. Lopes (#303732/2014-8) and N. H. Felício are thankful to CNPq and CAPES for the grants and financial support.

References

[1] M.-A. Gilles-Gonzalez, The smallest biomolecules: diatomics and their interactions with heme proteins, 1st ed., Elsevier Science, 2007.

[2] M.A. Gilles-Gonzalez, G. Gonzalez, Heme-based sensors: defining characteristics, recent developments, and regulatory hypotheses, J. Inorg. Biochem. 99 (2005) 1-22.

[3] T. Shimizu, D. Huang, F. Yan, M. Stranava, M. Bartosova, V. Fojtíková, M. Martínková, Gaseous O_2, NO, and CO in signal transduction: structure and function relationships of heme-based gas sensors and heme-redox sensors, Chem. Rev. 115 (2015) 6491-6533.

[4] M. Martínková, K. Kitanishi, T. Shimizu, Heme-based globin-coupled oxygen sensors: linking oxygen binding to functional regulation of diguanylate cyclase, histidine kinase, and methyl-accepting chemotaxis, J. Biol. Chem. 288 (2013) 27702-27711.

[5] M.-A. Gilles-Gonzalez, G.S. Ditta, D.R. Helinski, A hemoprotein with kinase activity encoded by the oxygen sensor of rhizobium meliloti, Nature 350 (1991) 170-172.

[6] M.-A. Gilles-Gonzalez, A.I. Caceres, E.H.S. Sousa, D.R. Tomchick, C. Brautigam, C. Gonzalez, M. Machius, A proximal arginine R206 participates in switching of the bradyrhizobium japonicum FixL oxygen sensor, J. Mol. Biol. 360 (2006) 80-89.

[7] C.M. Dunham, E.M. Dioum, J.R. Tuckerman, G. Gonzalez, W.G. Scott, M.-A. Gilles-Gonzalez, A distal arginine in oxygen-sensing heme-PAS domains is essential to ligand binding, signal transduction, and structure, Biochemistry 42 (2003) 7701-7708.

[8] J.R. Tuckerman, G. Gonzalez, E.M. Dioum, M.-A. Gilles-Gonzalez, Ligand and oxidation-state specific regulation of the heme-based oxygen sensor FixL from Sinorhizobium meliloti, Biochemistry 41 (2002) 6170-6177.

[9] J.R. Tuckerman, G. Gonzalez, M.-A. Gilles-Gonzalez, Complexation precedes phosphorylation for two-component regulatory system FixL/FixJ of Sinorhizobium meliloti, J. Mol. Biol. 308 (2001) 449-455.

[10] E.H.S. Sousa, G. Gonzalez, M.-A. Gilles-Gonzalez, Oxygen blocks the reaction of the FixL−FixJ complex with ATP but does not influence binding of FixJ or ATP to FixL, Biochemistry 44 (2005) 15359-15365.

[11] E.H.S. Sousa, J.R. Tuckerman, A.C.S. Gondim, G. Gonzalez, M.-A. Gilles-Gonzalez, Signal transduction and phosphoryl transfer by a FixL hybrid kinase with low oxygen affinity: importance of the vicinal PAS domain and receiver aspartate, Biochemistry 52 (2013) 456-465.

[12] E.H.S. Sousa, J.R. Tuckerman, G. Gonzalez, M.-A. Gilles-Gonzalez, A memory of oxygen binding explains the dose response of the heme-based sensor FixL, Biochemistry 46 (2007) 6249-6257.

[13] M. Mukai, K. Nakamura, H. Nakamura, T. Iizuka, Y. Shiro, Roles of Ile209 and Ile210 on the heme pocket structure and regulation of histidine kinase activity of oxygen sensor FixL from Rhizobium meliloti, Biochemistry 39 (2000) 13810-13816.

[14] J. Key, V. Šrajer, R. Pahl, K. Moffat, Time-resolved crystallographic studies of the heme domain of the oxygen sensor FixL: structural dynamics of ligand rebinding and their relation to signal transduction, Biochemistry 46 (2007) 4706-4715.

[15] M.-A. Gilles-Gonzalez, G. Gonzalez, Regulation of the kinase activity of heme protein FixL from the two-component system FixL/FixJ of Rhizobium meliloti, J. Biol. Chem. 268 (1993) 16293-16297.

[16] K.R. Rodgers, G.S. Lukat-Rodgers, Insights into heme-based O_2 sensing from structure–function relationships in the FixL proteins, J. Inorg. Biochem. 99 (2005) 963-977.

[17] C. Olea, E.M. Boon, P. Pellicena, J. Kuriyan, M.A. Marletta, Probing the function of heme distortion in the H-NOX family, ACS Chem. Biol. 3 (2008) 703-710.

[18] V. Balland, L. Bouzhir-Sima, E. Anxolabéhère-Mallart, A. Boussac, M.H. Vos, U. Liebl, T.A. Mattioli, Functional implications of the propionate 7−Arginine 220 interaction in the FixLH oxygen sensor from Bradyrhizobium japonicum, Biochemistry 45 (2006) 2072-2084.

[19] Y. Sasakura, S. Hirata, S. Sugiyama, S. Suzuki, S. Taguchi, M. Watanabe, T. Matsui, I. Sagami, T. Shimizu, Characterization of a direct oxygen sensor heme protein from Escherichia coli: effects of the heme redox states and mutations at the heme-binding site on catalysis and structure, J. Biol. Chem. 277 (2002) 23821-23827.

[20] K. Kitanishi, K. Kobayashi, Y. Kawamura, I. Ishigami, T. Ogura, K. Nakajima, J. Igarashi, A. Tanaka, T. Shimizu, Important roles of Tyr43 at the putative heme distal side in the oxygen recognition and stability of the Fe(II)−O_2 complex of YddV, a globin-coupled heme-based oxygen sensor diguanylate cyclase, Biochemistry 49 (2010) 10381-10393.

[21] M.L. Fultz, R.A. Durst, Mediator compounds for the electrochemical study of biological redox systems: a compilation, Anal. Chim. Acta 140 (1982) 1-18.

[22] I.I. Creaser, J.M. Harrowfield, A.J. Herlt, A.M. Sargeson, J. Springborg, R.J. Geue, M.R. Snow, Sepulchrate: a macrobicyclic nitrogen cage for metal ions, J. Am. Chem. Soc. 99 (1977) 3181-3182.

[23] J.I. Bruce, L.R. Gahan, T.W. Hambley, R. Stranger, Synthesis, structure, and spectroscopy of encapsulated complexes of cobalt(III) derived from the ligand 5-methyl-5-(4-amino-2-thiabutyl)-3,7-diazanonane-1,9-diamine (N5S), Inorg. Chem. 32 (1993) 5997-6002.

[24] T.M. Donlevy, L.R. Gahan, T.W. Hambley, R. Stranger, Synthesis and spectroscopic properties of the encapsulated cobalt(III) complexes derived from the unsymmetrically substituted ligand 5-methyl-5-(4-amino-2-azabutyl)-3,7-dithianonane-1,9-diamine (N4S2), Inorg. Chem. 31 (1992) 4376-4382.

[25] P.V. Bernhardt, A.M.T. Bygott, R.J. Geue, A.J. Hendry, B.R. Korybut-Daszkiewicz, P.A. Lay, J.R. Pladziewicz, A.M. Sargeson, A.C. Willis, Stabilization of cobalt cage conformers in the solid state and solution, Inorg. Chem. 33 (1994) 4553-4561.

[26] P.V. Bernhardt, G.A. Lawrance, T.W. Hambley, 6,13-Diamino-6,13-dimethyl-1,4,8,11-tetra-azacyclotetradecane, L7, a new, potentially sexidentate polyamine

ligand. Variable coordination to Cobalt (III) and crystal structure of the complex [Co(L7)]Cl_2[ClO_4], J. Chem. Soc., Dalton Trans. (1989) 1059-1065.

[27] R.J. Geue, T.W. Hambley, J.M. Harrowfield, A.M. Sargeson, M.R. Snow, Metal ion encapsulation: cobalt cages derived from polyamines, formaldehyde, and nitromethane, J. Am. Chem. Soc. 106 (1984) 5478-5488.

[28] M. Maeder, P. King, ReactLab REDOX, Jplus Consulting Pty Ltd, Perth, Western Australia, 2016.

[29] M. Maeder, P. King, ReactLab Kinetics,Vol. 1.1, Jplus Consulting Pty Ltd, Perth, Western Australia, 2012.

[30] P.V. Bernhardt, K.-I. Chen, P.C. Sharpe, Transition metal complexes as mediator-titrants in protein redox potentiometry, J. Biol. Inorg. Chem. 11 (2006) 930-936.

[31] M.-A. Gilles-Gonzalez,, G. Gonzalez, M.F. Perutz, L. Kiger, M.C. Marden, C. Poyart, Heme-based sensors, exemplified by the kinase FixL, are a new class of heme protein with distinctive ligand-binding and autoxidation, Biochemistry 33 (1994) 8067-8073.

[32] M.-A. Gilles-Gonzalez, G. Gonzalez, M.F. Perutz, Kinase-activity of oxygen sensor FixL depends on the spin-state of its heme iron, Biochemistry 34 (1995) 232-236.

[33] J.R. Tuckerman, G. Gonzalez, E.H.S. Sousa, X. Wan, J.A. Saito, M. Alam, M.-A. Gilles-Gonzalez, An oxygen-sensing diguanylate cyclase and phosphodiesterase couple for c-di-GMP control, Biochemistry 48 (2009) 9764-9774.

[34] V.M. Delgado-Nixon, G. Gonzalez, M.-A. Gilles-Gonzalez, Dos, a heme-binding PAS Protein from Escherichia coli, is a direct oxygen sensor, Biochemistry 39 (2000) 2685-2691.

[35] S. Hirata, T. Matsui, Y. Sasakura, S. Sugiyama, T. Yoshimura, I. Sagami, T. Shimizu, Characterization of Met95 mutants of a heme-regulated phosphodiesterase from Escherichia coli, Eur. J. Biochem. 270 (2003) 4771-4779.

[36] Y. Ishitsuka, Y. Araki, A. Tanaka, J. Igarashi, O. Ito, T. Shimizu, Arg97 at the heme-distal side of the isolated heme-bound PAS domain of a heme-based oxygen sensor from Escherichia coli (Ec DOS) plays critical roles in autoxidation and binding to gases, particularly O_2, Biochemistry 47 (2008) 8874-8884.

[37] B.G. Fritz, X. Hu, J.L. Brailey, R.E. Berry, F.A. Walker, W.R. Montfort, Oxidation and loss of heme in soluble guanylyl cyclase from Manduca sexta, Biochemistry 50 (2011) 5813-5815.

[38] R. Makino, S.-y. Park, E. Obayashi, T. Iizuka, H. Hori, Y. Shiro, Oxygen binding and redox properties of the heme in soluble guanylate cyclase: implications for the mechanism of ligand discrimination, J. Biol. Chem. 286 (2011) 15678-15687.

[39] S. Yoshioka, K. Kobayashi, H. Yoshimura, T. Uchida, T. Kitagawa, S. Aono, Biophysical properties of a c-type heme in chemotaxis signal transducer protein DcrA, Biochemistry 44 (2005) 15406-15413.

[40] P.R. Pokkuluri, M. Pessanha, Y.Y. Londer, S.J. Wood, N.E.C. Duke, R. Wilton, T. Catarino, C.A. Salgueiro, M. Schiffer, Structures and solution properties of two novel periplasmic sensor domains with c-type heme from chemotaxis proteins of geobacter sulfurreducens: implications for signal transduction, J. Mol. Biol. 377 (2008) 1498-1517.

[41] B.C. King, F.M. Hawkridge, B.M. Hoffman, Electrochemical studies of cyanometmyoglobin and metmyoglobin: implications for long-range electron transfer in proteins, J. Am. Chem. Soc. 114 (1992) 10603-10608.

[42] D.L. Johnson, B.C. Lewis, D.J. Elliot, J.O. Miners, L.L. Martin, Electrochemical characterisation of the human cytochrome P450 CYP2C9, Biochem. Pharmacol. 69 (2005) 1533-1541.

[43] A.B. Cowley, M.L. Kennedy, S. Silchenko, G.S. Lukat-Rodgers, K.R. Rodgers, D.R. Benson, Insight into heme protein redox potential control and functional aspects of six-coordinate ligand-sensing heme proteins from studies of synthetic heme peptides, Inorg. Chem. 45 (2006) 9985-10001.

[44] H.M. Marques, I. Cukrowski, P.R. Vashi, Coordination of weak field ligands by *N*-acetylmicroperoxidase-8 (NAcMP8), a ferric haempeptide from cytochrome *c*, and the influence of the axial ligand on the reduction potential of complexes of NAcMP8, J. Chem. Soc., Dalton Trans. (2000) 1335-1342.

[45] W.C. Winkler, G. Gonzalez, J.B. Wittenberg, R. Hille, N. Dakappagari, A. Jacob, L.A. Gonzalez, M.-A. Gilles-Gonzalez, Nonsteric factors dominate binding of nitric oxide, azide, imidazole, cyanide, and fluoride to the rhizobial heme-based oxygen sensor FixL, Chem. Biol. 3 (1996) 841-850.

[46] J. Key, K. Moffat, Crystal structures of deoxy and CO-Bound *Bj*FixLH reveal details of ligand recognition and signaling, Biochemistry 44 (2005) 4627-4635.

[47] B. Hao, C. Isaza, J. Arndt, M. Soltis, M.K. Chan, Structure-based mechanism of O_2 sensing and ligand discrimination by the FixL heme domain of Bradyrhizobium japonicum, Biochemistry 41 (2002) 12952-12958.

[48] W. Gong, B. Hao, M.K. Chan, New mechanistic insights from structural studies of the oxygen-sensing domain of Bradyrhizobium japonicum FixL, Biochemistry 39 (2000) 3955-3962.

[49] H. Miyatake, M. Mukai, S.-Y. Park, S.-i. Adachi, K. Tamura, H. Nakamura, K. Nakamura, T. Tsuchiya, T. Iizuka, Y. Shiro, Sensory mechanism of oxygen sensor

FixL from Rhizobium meliloti: crystallographic, mutagenesis and resonance raman spectroscopic studies, J. Mol. Biol. 301 (2000) 415-431.

[50] W. Gong, B. Hao, S.S. Mansy, G. Gonzalez, M.-A. Gilles-Gonzalez, M.K. Chan, Structure of a biological oxygen sensor: a new mechanism for heme-driven signal transduction, Proc. Natl. Acad. Sci. U. S. A. 95 (1998) 15177-15182.

[51] E. Lloyd, D.L. Burk, J.C. Ferrer, R. Maurus, J. Doran, P.R. Carey, G.D. Brayer, A.G. Mauk, Electrostatic modification of the active site of myoglobin: characterization of the proximal Ser92Asp variant, Biochemistry 35 (1996) 11901-11912.

[52] A.R. Lim, B.P. Sishta, A. Grant Mauk, Contribution of the heme propionate groups to the electron transfer and electrostatic properties of myoglobin, J. Inorg. Biochem. 100 (2006) 2017-2023.

Graphical abstract

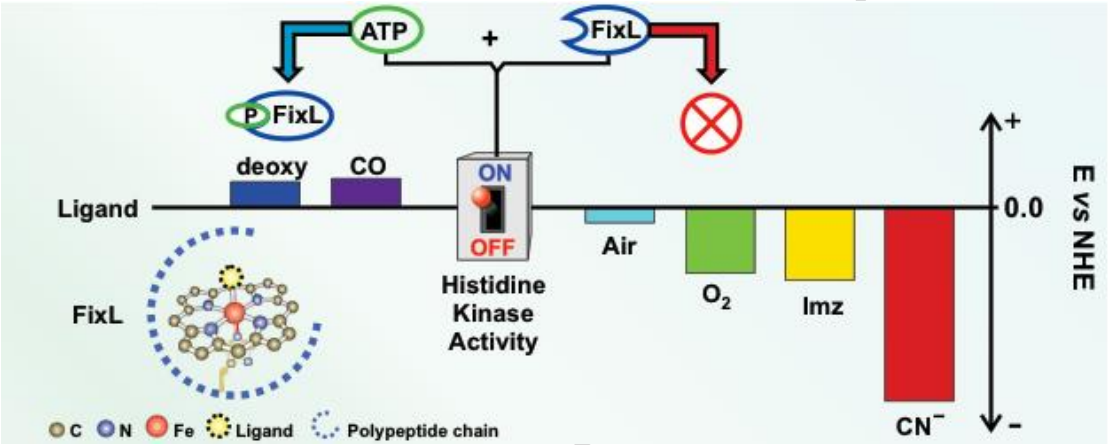

Graphical Abstract (synopsis)

Midpoint potentials assigned to the $Fe^{III/II}$ redox couple of the heme domain of FixL from *Rhizobium etli* (*Re*FixL) were determined for the unliganded state (+19 mV) and bounded to CO (+21 mV), O_2 (–51 mV), imidazole (–57 mV) and CN^- (–156 mV) and support a correlation with the kinase activity.

Highlights

- First time measured the electrochemical potential of a full-length FixL protein
- Potentials were determined for *Rhizobium etli* FixL (*Re*FixL) bounded to different ligands
- Surprisingly, oxygen bound *Re*FixL showed a negative potential shift of 70 mV
- Electrochemical potentials showed a trend linked to the histidine-kinase activity